3D Mesh Skeleton Extraction Using Topological and Geometrical Analyses

Julien Tierny, Jean-Philippe Vandeborre, Mohamed Daoudi

3D Mesh Skeleton Extraction Using Topological and Geometrical Analyses

Julien Tierny, Jean-Philippe Vandeborre* and Mohamed Daoudi*

FOX-MIIRE Research Group – LIFL (UMR USTL/CNRS 8022)
* GET / INT / Télécom Lille 1, France
{*tierny, vandeborre, daoudi*}*@lifl.fr*

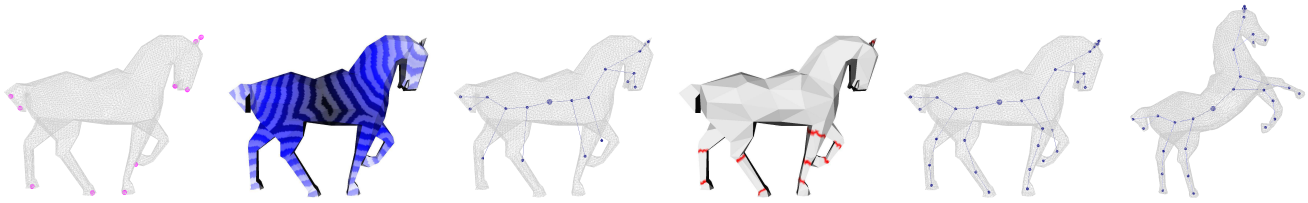

(a) Feature points. (b) Mapping function. (c) Dual Reeb graph. (d) Constriction approximation. (e) Constriction enhanced graph. (f) Application to deformation.

Figure 1. Main steps of presented method on a standard model.

Abstract

This paper describes a novel and unified approach for Reeb graph construction and simplification as well as constriction approximation on 3D polygonal meshes. The key idea of our algorithm is that discrete contours *– curves carried by the edges of the mesh and approximating the continuous contours of a mapping function – encode both topological and geometrical shape characteristics.*

Firstly, mesh feature points are computed. Then they are used as geodesic origins for the computation of an invariant mapping function that reveals the shape most significant features. Secondly, for each vertex in the mesh, its discrete contour *is computed. As the set of* discrete contours *recovers the whole surface, each of them can be analyzed, both to detect topological changes or constrictions. Constriction approximations enable Reeb graphs refinement into more visually meaningful skeletons, that we refer as* enhanced topological skeletons.

Without pre-processing stages and without input parameters, our method provides nice-looking and affine-invariant skeletons, with satisfactory execution times. This makes enhanced topological skeletons good candidates for applications needing high level shape representations, such as mesh deformation (experimented in this paper), retrieval, compression, metamorphosis, etc.

1. Introduction

Polygonal mesh is a widely used representation of 3D shapes, mainly for exchange and display purposes. However, many applications in computer graphics need higher level shape descriptions as an input. Topological skeletons have shown to be interesting shape descriptions [2]. They benefit diverse fields like shape metamorphosis, deformation [13], retrieval [10], texture mapping, etc.

Many topological approaches study the properties of real valued functions computed over triangulated surfaces. Most of the time, those functions are provided by the application context, such as scientific data analysis [4]. When dealing with topological skeletons, it is necessary to define an invariant and visually interesting mapping function, which remains an open issue [2].

Moreover, traditional topological graph construction algorithms assume that all the information brought by the mapping function is pertinent, while in practice, this can lead to large graphs [18, 5], encoding noisy details.

Finally, topological approaches cannot discriminate visually interesting sub-parts of identified connected components, like the phalanxes of a finger. This is detrimental to certain applications, such as mesh deformation.

In this paper, we propose a novel and unified method which addresses the above issues. Given a connected triangulated surface T, feature points are firstly extracted (fig. 1(a)) in order to compute an invariant mapping function, noted f_m (fig. 1(b)), which reveals the shape most signifi-

cant parts. Secondly, for each vertex in the mesh, we compute its *discrete contour*, a connected curve traversing it and locally minimizing f_m gradient. We show that a topological analysis of those *discrete contours* enables a pertinent Reeb graph construction and simplification (fig. 1(c)), without any input parameter. Finally, we show that a geometrical analysis of *discrete contours* can approximate constrictions on prominent components (fig. 1(d)), enabling the refinement of Reeb graphs into enhanced topological skeletons (fig. 1(e)).

This paper is structured as follows. Firstly, we introduce topological skeleton related work. Secondly, we define our mapping function f_m. Thirdly, we present our algorithm for *discrete contour* computation, which is used both for the Reeb graph construction and simplification as well as the constriction approximation. Finally, we comment on experimental results and discuss about possible applications, like mesh deformation (fig. 1(f)).

2. Related work

Several approaches have been explored for the decomposition of polygonal meshes into meaningful subcomponents, to extract skeletal representations of shapes.

In comparison to mesh segmentation [20] and traditional skeleton extraction [3, 24], topological approaches, based on Morse and Reeb graph theories [16, 19, 15], present the advantage to preserve the topological properties of the shape [2] (number of loops, number and relations between components, etc.). However, with regard to shape skeletons, we identify three main drawbacks in topological approaches, successively addressed in this paper.

Firstly, it is difficult to define an invariant and visually interesting mapping function. Secondly, constructing and transforming a topological graph into a manageable skeleton is not a trivial problem. Finally, topological approaches decompose a surface into connected sub-components only. This means that visually interesting sub-parts of identified connected components will not be discriminated: for example, a finger of a hand model will not be decomposed into phalanxes.

2.1. Mapping functions

Differential topology based approaches study the properties of real valued functions, that we refer as *mapping functions*, defined on input surfaces, either to construct Reeb graphs [22, 6], contour trees [5], level set diagrams [12] or Morse complexes [18, 4]. Those functions are often brought by the application context: terrain modeling [22], MRI analysis [5], molecular analysis [4], etc.

When dealing with topological skeletons, it is necessary to define a scalar function which satisfies invariance and stability constraints, and which also affords a topological description that highlights visually significant surface subcomponents.

Lazarus and Verroust [12] introduced such a function, defined by the *geodesic distance* (the length of the shortest path between vertices) from a source vertex to any other vertex in the mesh. It leads to visually interesting results for natural objects because it is invariant to geometrical transformations and it is robust against variations in model pose [11]. Due to a lack of stability, within the framework of shape retrieval, Hilaga et al. [10] proposed to integrate this function all over the mesh. Unfortunately, from our experience, that function generates an important amount of critical points, configurations where the gradient of the function vanishes, which makes the construction of visually meaningful graphs more complex.

In our method, to reveal the shape most significant features, we focus on feature points. Feature points are mesh vertices located on extremities of prominent components [11]. Mortara and Patanè [17] proposed to select as feature points the vertices where Gaussian curvature exceeds a given threshold, but this cannot resolve extraction on constant curvature areas. Katz et al. [11] developed an algorithm based on multi-dimensional scaling in quadratic execution complexity. In this paper, we propose a robust and straightforward algorithm for feature point extraction (fig. 1(a)). Moreover, we use them as geodesic origins for the definition of our mapping function (fig. 1(b)). Such a function well reveals the most visually significant parts of the mesh, generating manageable critical point sets.

2.2. Graph construction and simplification

A Reeb graph [19] is a topological structure that encodes the connectivity relations of the critical points of a scalar function defined on an input surface. More formally, Reeb graphs are defined as follows:

Definition 1 (Reeb graph) *Let $f : M \rightarrow \mathbb{R}$ be a scalar function defined on a compact manifold M. The Reeb graph of f is the quotient space of f in $M \times \mathbb{R}$ by the equivalence relation $(p_1, f(p_1)) \sim (p_2, f(p2))$, if and only if:*

$$\begin{cases} f(p_1) = f(p_2) \\ p_1 \text{ and } p_2 \text{ belong to the same connected} \\ \qquad \text{component of } f^{-1}(f(p_1)) \end{cases}$$

Figure 2 gives an example of a Reeb graph computed on a bi-torus with regard to the height function and well illustrates the fact that Reeb graphs can be used as skeletons.

Constructing a Reeb graph from a scalar function f computed on a triangulated surface first requires to identify the set of vertices corresponding to critical points. With this aim, several formulations have been proposed [7, 23] to identify local maxima, minima and saddles, observing for each vertex the evolution of f at its direct neighbors. Several algorithms have been developed to construct

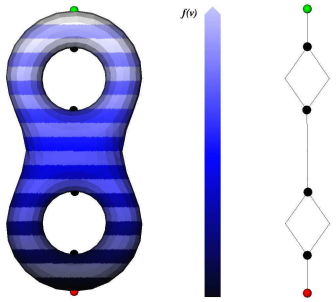

Figure 2. Evolution of the level lines of the height function on a bi-torus, its critical points and its Reeb graph.

Reeb graphs from the connectivity relations of these critical points [6, 5], most of them in $O(n \times log(n))$ steps, with n the number of vertices in the mesh. However, they assume that all the information brought by the scalar function f is relevant [18, 5]. Consequently, they assume that all the identified critical points are meaningful, while in practice, this hypothesis can lead to unmanageably large Reeb graphs. To overcome this issue, Ni et al. [18] developed a user-controlled simplification algorithm. Bremer et al. [4] proposed an interesting critical point cancellation technique based on a *persistence* threshold. Attene et al. [1] proposed a seducing approach, unifying the graph construction and simplification, but it is conditioned by a *slicing* parameter.

In this paper, we propose a discrete formulation of contours, connected subsets of level lines, which enables, without any input parameter, the construction of visually meaningful Reeb graphs (fig. 1(c)).

2.3. Constriction computation

Hétroy and Attali [9] define constrictions as simple closed curves, whose length is locally minimal. Constrictions are located on the narrowest parts of a surface. This notion is of major interest for segmenting individual subcomponents identified with standard topological approaches into more significant parts, for deformation purpose for example. Recently, Hétroy [8] showed that constriction detection could be achieved by analyzing surface curvature.

In this paper, we propose to analyze the geometrical characteristics of discrete contours, and particularly their concavity, to approximate constrictions (fig. 1(d)), in order to decompose previously identified components into more visually interesting parts (fig. 1(e)).

3. Method overview

Given a connected triangulated surface T, we propose in this paper a unified method to decompose T into visually meaningful sub-parts, considering the topological and geometrical characteristics of *discrete contours*.

The algorithm proceeds in three stages. Firstly, mesh feature points are extracted (fig. 1(a)) in order to compute an invariant and visually interesting mapping function (fig. 1(b)), denoted f_m in the rest of the paper. Secondly, for each vertex in the mesh, we compute its *discrete contour*, a curve traversing it and approximating f_m continuous contour. Finally, as the set of *discrete contours* recovers the entire mesh, it is possible to analyze each contour characteristics, either to detect topological changes (fig. 1(c)) or to detect curvature transitions (fig. 1(d)).

Our scientific contribution resides in three points. *(i)* We propose an original and straightforward algorithm for feature point extraction. It can resolve extraction on constant curvature areas – such as spheres – and it is robust against variations in mesh sampling and model pose. *(ii)* We show that a *discrete contour* formulation enables, without re-meshing and without any input parameter, a pertinent Reeb graph construction, providing visually meaningful graphs, affine-invariant and robust to variations in mesh sampling. *(iii)* We show that the geometrical information brought by *discrete contours* enables the approximation of constrictions on prominent components and consequently Reeb graph refinement.

4. Mapping function

To compute visually meaningful topological skeletons, we first have to define a mapping function that will highlight the most significant parts of the mesh. In order to fit application constraints, this function has to present stability and invariance properties. Geodesic distances are affine-invariant and robust to variations in model pose. From an algorithmic point of view, they can be approximated by the Moore-Dijkstra algorithm (distance minimizing in weighted graphs). In the rest of this paper, we will refer to $\delta(v_1, v_2)$ as the normalized approximation of the geodesic distance from vertex v_1 to vertex v_2, normalized with regard to mesh global extrema.

4.1. Feature point extraction

Feature points are mesh vertices located on extremities of prominent components. As they highlight the most significant features of the shape, they are used in our mapping function computation as origins for geodesic distance evaluation. To extract them, we propose a quite straightforward algorithm, based on topological tools. Most of the geodesic based mapping function local extrema appear at extremities of prominent components (figs. 3(a) and 3(b)), mainly because gradient vanishes in those configurations. Therefore, we propose to realize a crossed analysis, using two geodesic based mapping functions – whose origins are the mesh most distant vertices – and to intersect the sets of their local extrema.

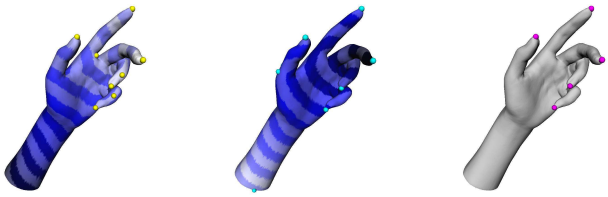

(a) E_1. (b) E_2. (c) $E_1 \cap E_2$.

Figure 3. Feature point extraction overview.

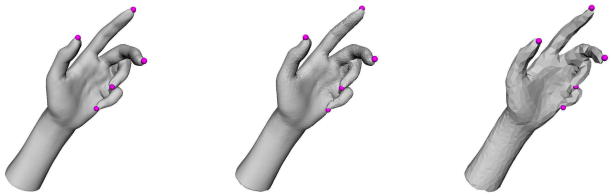

(a) 25 000 vertices. (b) 5 000 vertices. (c) 1 000 vertices.

Figure 4. Feature point extraction robustness against mesh sampling variations.

Let v_{s_1} and v_{s_2} be the most geodesic distant vertices of a connected triangulated surface T, computed with the Tree Diameter algorithm [12]. In figure 3, v_{s_1} is located at the extremity of the wrist (fig. 3(a)) while v_{s_2} is located at the extremity of the middle finger (fig. 3(b)).

Let f_{g_1} and f_{g_2} be two scalar functions defined on each vertex v of T, as follows:

$$f_{g_1}(v) = \delta(v, v_{s_1}) \quad (1)$$

$$f_{g_2}(v) = \delta(v, v_{s_2}) \quad (2)$$

Basing on the critical point classification proposed in [6], a *local minimum* is defined as a vertex such that all its direct neighbors have an upper function value. Reciprocally, we define a *local maximum* as a vertex such that all its direct neighbors have a lower function value. Let E_1 be the set of local extrema (minima and maxima) of f_{g_1} (in yellow in fig. 3(a)) and E_2 be the set of local extrema of f_{g_2} (in cyan in fig. 3(b)). Extremities of prominent components are configurations where f_{g_1} and f_{g_2} tend to an extremum (figs. 3(a) and 3(b)). Consequently, the set of feature points is both included in E_1 and E_2. Therefore, we define the set of feature points F of T (fig. 3(c)) as follows:

$$F = E_1 \cap E_2 \quad (3)$$

In practice, f_{g_1} and f_{g_2} local extrema which correspond to feature points do not appear exactly on the same vertices but in the same *geodesic neighborhood*. Therefore, the intersection constraint is relaxed as follows, with $\epsilon \in [0, 1]$ the radius of the *geodesic neighborhood* (geodesic distance are normalized):

$$v \in F \Longleftrightarrow \begin{cases} \exists v_{e_1} \in E_1 \quad / \quad \delta(v, v_{e_1}) < \epsilon \\ \exists v_{e_2} \in E_2 \quad / \quad \delta(v, v_{e_2}) < \epsilon \\ \delta(v, v_{f_i}) > \epsilon \quad \forall v_{f_i} \in F \\ \epsilon \in [0, 1] \end{cases} \quad (4)$$

From our experience, using only two geodesic mapping functions (f_{g_1} and f_{g_2}) and setting $\epsilon = 0.05$ give accurate results. Moore-Dijkstra's algorithm is a time complexity bottleneck. f_{g_1} and f_{g_2} are computed each in $O(n \times log(n))$ steps, with n the number of vertices in T.

In this paragraph, we presented a straightforward algorithm for mesh feature point extraction, in $O(n \times log(n))$ steps, with n the number of vertices in T. This algorithm is based on geodesic distance evaluations. Therefore it is stable and invariant to geometrical transformations and robust to variations in model pose. Furthermore, in order to select feature points, the mapping function gradient is analyzed. No hypothesis is required about mesh sampling. Consequently, this algorithm is robust against variations in mesh sampling, as illustrated in figure 4: feature points are similar when the resolution decreases. Moreover, it achieves correct extraction on constant curvature areas, such as spheres, as shown in fig. 5(a).

4.2. Mapping function computation

When dealing with topological skeletons, it is necessary to define an invariant and visually interesting mapping function, which reveals the most significant parts of the mesh. Moreover, the mapping function should not generate an unmanageable set of critical points, in order to make the graph simplification easier. From our experience, this is not the case of the function presented in [10].

Firstly, to guarantee invariance to geometrical transformations and robustness against variations in model pose, geodesic distances are used. Secondly, to define a visually interesting mapping function, feature points are taken as origins for geodesic distance evaluations. Therefore, we propose the following mapping function, noted f_m in the rest of the paper, which computes in each vertex v of T the geodesic distance to the closest feature point:

$$f_m(v) = \frac{f_c(v) - min_{v \in T} f_c(v)}{max_{v \in T} f_c(v) - min_{v \in T} f_c(v)} \quad (5)$$

f_m is a normalized version of the function f_c, defined as follows ($f_c(v) \geq 0, \forall v \in T$):

$$f_c(v) = 1 - \delta'(v, v_c) \quad (6)$$

with v_c the closest feature point from v:

$$v_c \in F \quad / \quad \delta'(v, v_c) = min_{v_{f_i} \in F} \quad \delta(v, v_{f_i}) \quad (7)$$

Notice that f_m is invariant to uniform scaling (thanks to the normalization), rotation and translation (thanks to the use of geodesic distances). Figure 5 presents some computations of f_m over arbitrary shapes, the number of extracted feature points ($|F|$) and the number of critical points ($|C|$, identified according to the classification proposed in [6]). f_m has been defined so as it tends to maxima (in green) at

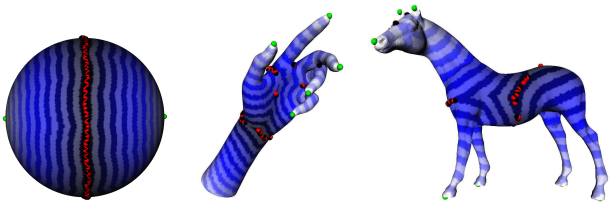

(a) $|F| = 2$, $|C| = 326$. (b) $|F| = 6$, $|C| = 94$. (c) $|F| = 7, |C| = 92$.

Figure 5. f_m mapping function computed on arbitrary shapes.

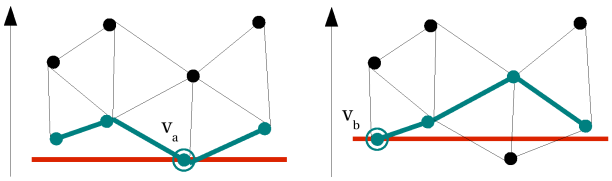

(a) $\Gamma(v_a)$. (b) $\Gamma(v_b)$.

Figure 6. Example of continuous (red) and discrete (green) level lines (height function).

feature points and it tends to minima (in red) at the center of the object.

As shown in figure 5, f_m generates an important number of critical points. Consequently, standard Reeb graph construction algorithms would create large graphs, counting as many nodes as critical points, which is a major issue for topological skeleton extraction. In the next section, we present a formulation of *discrete contours*, which enables a unified graph construction and simplification process.

5. Discrete contours of a mapping function

In this section, we propose to construct *discrete contours*. In the next sections, those *discrete contours* will be used either to detect topological changes or to detect curvature transitions, providing enhanced topological skeletons, without re-meshing and without any input parameter.

Defining contours of a real function f computed on a triangulated surface T is not a simple problem. In the continuous case, two points p_1 and p_2 belong to the same level line $f^{-1}(f(p_1))$ if $f(p_2) - f(p_1) = 0$. Moreover, p_1 and p_2 belong to the same *contour* if they belong to the same connected component of $f^{-1}(f(p_1))$.

In the discrete case, for a given vertex $v \in T$, depending on T sampling, $f^{-1}(f(v))$ is often reduced to the vertex v itself. With regard to definition 1, a correct Reeb graph could not be constructed from this formulation of discrete contours, because the conditions of the equivalence relation would rarely be satisfied.

To preserve contour topological properties in the discrete case, we define the *discrete level line* $\Gamma(v)$ associated to the vertex v as a curve computed along the edges of T which approximates by upper value the continuous level line $f^{-1}(f(v))$. Figure 6 shows *discrete level lines* traversing an arbitrary triangulation, with regard to the height function. Moreover, each connected subset of a *discrete level line* is referred as a *discrete contour*. In particular, we define the *discrete contour* $\gamma(v)$ associated to the vertex v as the connected subset of $\Gamma(v)$ containing v. Notice that the more T will be dense, the more *discrete contours* will tend to continuous contours.

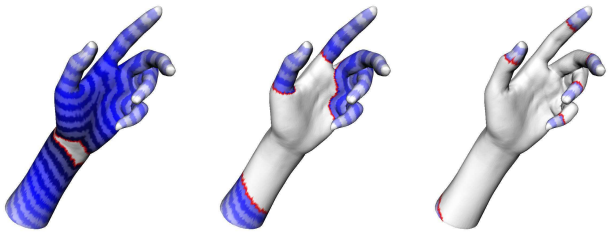

(a) $\Gamma(v_{600})$, 2 contours. (b) $\Gamma(v_{10\ 000})$, 4 contours. (c) $\Gamma(v_{20\ 000})$, 6 contours.

Figure 7. Example of discrete level lines on a 25 000 vertex mesh (f_m function).

Discrete contours can be computed for the whole mesh using a step by step gradient ascent process, described in algorithm 1. It handles two heaps, respectively the set of visited vertices Vt and the set of candidate vertices for visit Cd. At each step, Cd surrounds Vt by upper value.

Algorithm 1 Discrete contour computation.

$Vt = \emptyset$
$Cd \leftarrow \{argmin_{v' \in T} f(v')\}$
while $Cd \neq \emptyset$ **do**
  $v \leftarrow argmin_{v' \in Cd} f(v')$
  $\Gamma(v) \leftarrow Cd$
  $\gamma(v) \leftarrow$ connected subset of Cd, containing v
  Remove v from Cd
  $Cd \leftarrow Cd \cup \{v$ neighbors, which are not in $Vt\}$
  Add v to Vt
end while

A *discrete level line* locally minimizes its *difference* with the continuous level line it approximates. This difference can be expressed as follows:

$$\sum_{v_i \in \Gamma(v)} (f(v_i) - f(v)) \quad / \quad f(v_i) \geq f(v), \forall v_i \in \Gamma(v) \quad (8)$$

In expression 8, $f(v)$ is a constant term. Consequently, minimizing this expression is equivalent to minimizing $f(v_i)$ which is actually performed at each iteration of algorithm 1. Cd always surrounds Vt by upper value and minimizes expression 8, thus it is equivalent to $\Gamma(v)$.

In figure 7, examples of discrete level lines $\Gamma(v_i)$ are

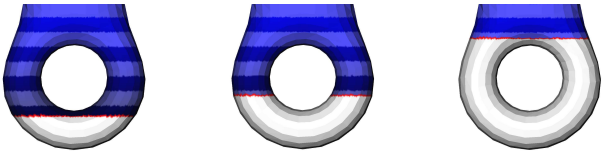

(a) 1 contour. (b) 2 contours. (c) 1 contour.

Figure 8. Bifurcation and junction contexts on a torus shape (height function).

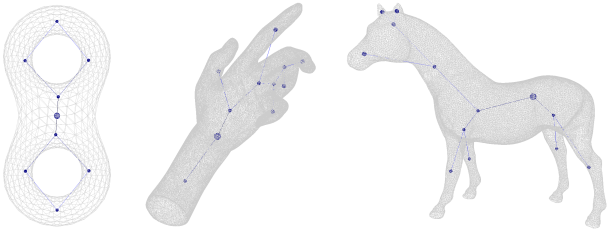

(a) (b) (c)

Figure 9. Dual Reeb graphs of primitive and complex shapes (f_m function).

shown, at different iterations i of the algorithm. Vt vertex set is displayed in white and $\Gamma(v)$ is displayed in red. Visiting in a recursive fashion each vertex of $\Gamma(v)$ enables the identification of each of its connected subsets, and particularly $\gamma(v)$.

6. Topological analysis of discrete contours

Standard Reeb graph construction algorithms need simplification in order to remove noisy details. In this section, we propose a unified algorithm for graph construction and simplification, based on the topological analysis of discrete contours. Following the definition 1 of a Reeb graph in the continuous case, we can state an analog equivalence relation in the discrete case between two vertices $v_1, v_2 \in T$, based on our notion of discrete contour:

$$(v_1, f(v_1)) \sim (v_2, f(v_2)) \Longleftrightarrow \begin{cases} v_2 \in \Gamma(v_1) \\ v_2 \in \gamma(v_1) \end{cases} \quad (9)$$

v_1 and v_2 belong to the same connected component if they satisfy the above conditions. Therefore, at each iteration of the contour computation algorithm, each individual connected component of T, traversed by $\Gamma(v)$, can be identified. Thus, topological changes can be detected observing the number $N_{\Gamma(v)}$ of connected subset of $\Gamma(v)$, as f evolves. We define three types of topological changes:

1. *bifurcations*: when $N_{\Gamma(v)}$ increases from iteration t to iteration $t+1$ ($\Gamma(v)$ splits in two contours from 8(a) to 8(b)),
2. *junctions*: when $N_{\Gamma(v)}$ decreases from t to $t+1$ and when several discrete contours merge (two contours merge in one from 8(b) to 8(c)),

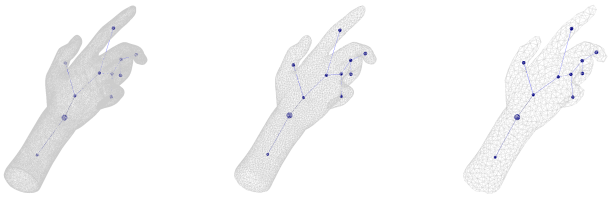

(a) 25 000 vertices. (b) 5 000 vertices. (c) 1 000 vertices.

Figure 10. Algorithm robustness against mesh sampling variations.

3. *terminations*: when $N_{\Gamma(v)}$ decreases from t to $t+1$, without discrete contour merge.

Figure 9 shows several dual Reeb graphs obtained with this strategy, with regard to f_m. Connected components are represented by the nodes located at their barycenter.

The main contribution of our algorithm is that graph construction and simplification are performed at the same time. If we compare figures 9 and 5, we notice that the dual Reeb graphs do not reflect the presence of noisy critical points (points in red in figure 5), because discrete level lines do not disconnect in those configurations. Standard Reeb graph algorithms would have generated graphs counting as many nodes as critical points – 94 nodes for the hand model and 92 nodes for the horse model – while in our approach only meaningful topological variations are encoded in the graph.

In comparison to [1, 10], no re-meshing and no input parameter, such as a *slicing* parameter, are required. Consequently, as no assumption is made about T sampling, this algorithm is robust against variations in mesh sampling, as shown in fig. 10. Furthermore, as f_m is based on normalized geodesic distance evaluations, presented graphs are also invariant to geometrical transformations (rotation, translation and uniform scaling).

In this section, we presented a unified graph construction and simplification algorithm, based on the topological analysis of *discrete contours*. As contours do not disconnect in f_m noisy parts, resulting graphs reveal the shape most significant features. However, a strict topological analysis cannot discriminate visually meaningful sub-parts of a given connected component. To overcome this issue, we propose in the next section to analyze the geometrical characteristics of *discrete contours* to detect constrictions.

7. Geometrical analysis of discrete contours

Constriction approximations enable the subdivision of the branches of topological skeletons into more visually interesting parts. In this section, we propose an algorithm for constriction approximation, based on the analysis of the curvature of *discrete contours*. For each *discrete contour* identified in the previous stage, we compute its Gaussian curvature and we identify local minima as constrictions.

Model	$f_\tau = 3$	$f_\tau = 5$	$f_\tau = 10$	$f_\tau = 15$
Humanoid	4	8	9	12
Horse 1	11	11	11	12
Hand 1	5	8	11	12
Hand 2	6	9	11	11
Horse 2	9	14	19	19

Table 1. Number of constrictions with different concavity curve cutoff frequencies (f_τ).

7.1. Topological constraint

Since constrictions are defined as closed curves, the analysis has to be restricted on *closed* discrete contours only. Considering each contour $\gamma(v)$ as a connected and non-directed planar graph G, $\gamma(v)$ is a cycle, and consequently a closed curve, if the degree of all its vertices equals two. Therefore for each discrete contour of T reduced to a planar graph G, the degree of each of its vertex is computed and we only consider in the rest of our algorithms contours that satisfy the above property.

7.2. Concavity curves

In our experiments, the average curvature $\zeta(\gamma(v))$ of each *discrete contour* $\gamma(v)$ is estimated by computing the Discrete Gaussian Curvature [14] in each of its vertex. If $\zeta(\gamma(v))$ is positive, $\gamma(v)$ neighborhood is globally convex, otherwise it is concave. Constrictions appear on the narrowest, or the most concave, parts of a surface. Consequently, in order to only consider concave discrete contours, we compute $\zeta'(\gamma(v))$ as follows:

$$\zeta'(\gamma(v)) = \begin{cases} \zeta(\gamma(v)) & \text{if} \quad \zeta(\gamma(v)) \leq 0 \\ 0 & \text{if} \quad \zeta(\gamma(v)) > 0 \end{cases} \tag{10}$$

During the discrete contour computation, each contour is stored in the related node of the dual Reeb graph. As this algorithm visits T from the lowest to the highest f_m values, for a given node of the graph, contours are automatically sorted by f_m values. Computing $\zeta'(\gamma(v))$ sequentially for each of these sorted contours gives, for a given node, a *concavity curve*, an overview of the concavity evolution as f_m evolves.

Curves shown in figure 11 give examples of such evolutions, computed on the neck of the horse model (fig. 12(j)). The left values of these *concavity curves* correspond to the concavity estimations of the discrete contours located at the basis of the neck. The right values correspond to the concavity estimations of the discrete contours located at the end of the neck (basis of the head sub-part).

7.3. Constriction approximation

Curvature is a well-known noise sensitive entity. Consequently, to compute nice-looking approximations of constrictions, we have to reduce high frequency noise in concavity curves. Reducing noise on a one-dimensional data

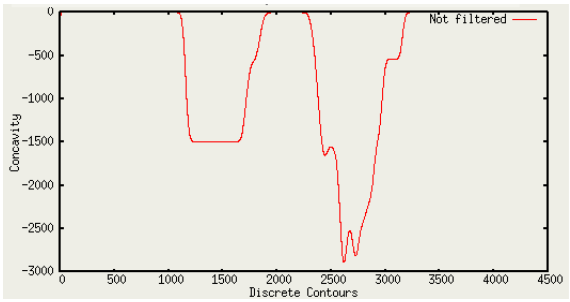

(a) Unfiltered curve.

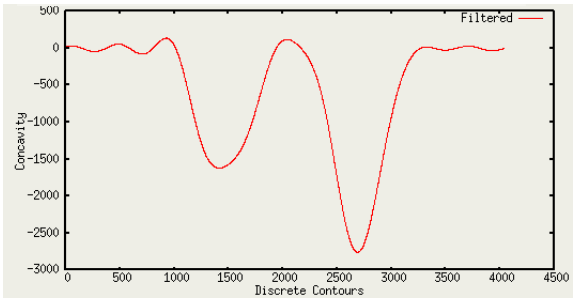

(b) Filtered curve ($f_\tau = 10$).

Figure 11. Concavity curves for the neck of the horse model (unfiltered and filtered).

set is a trivial signal-processing problem. This can be achieved by applying an ideal low-pass filter of cutoff frequency f_τ, defined by the following transfer function:

$$H(f_{\gamma(v)}) = \begin{cases} 1 & \text{if} \quad f_{\gamma(v)} \leq f_\tau \\ 0 & \text{if} \quad f_{\gamma(v)} > f_\tau \end{cases} \tag{11}$$

A filtered version of $\zeta'(\gamma(v))$ is given by the following expression, where FT stands for the Fourier Transform:

$$\widehat{\zeta'}(\gamma(v)) = FT^{-1}(H(f_{\gamma(v)}) \times FT(\zeta'(\gamma(v)))) \tag{12}$$

As shown in figure 11(b), low-pass filtering enables the discrimination of strongly concave contours. Consequently, for each node of the topological skeleton, we identify as constriction approximations the discrete contours that strongly minimize $\widehat{\zeta'}(\gamma(v))$. Then, the dual Reeb graph is refined, subdividing each node using its constrictions as boundaries between sub-parts.

8. Experiments and results

In this section, we present and comment on experimental results obtained with our method and we discuss about its applications, particularly mesh deformation. Presented models are connected triangulated surfaces extracted from the *Princeton Shape Benchmark* database [21].

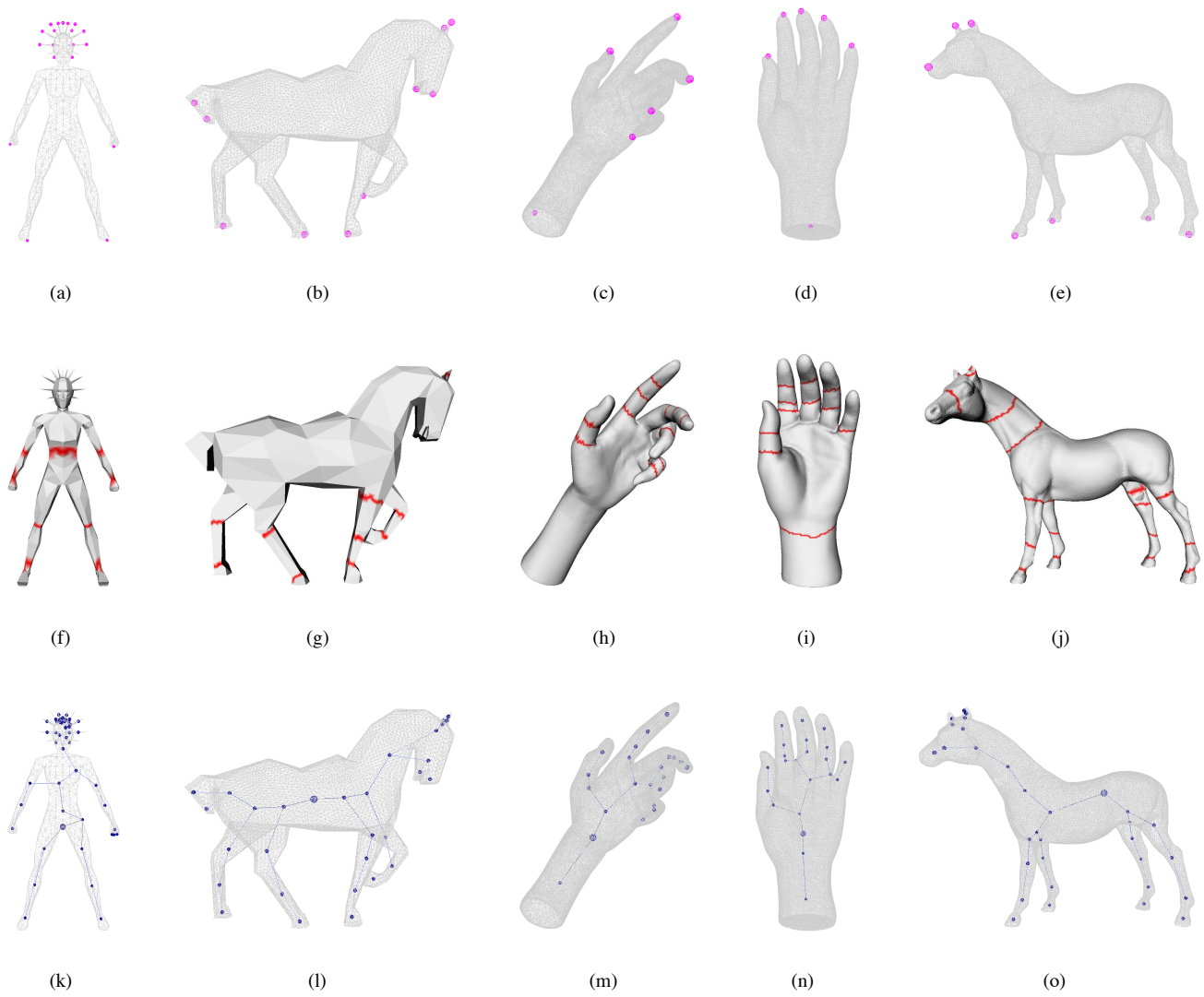

Figure 12. Feature points, constriction approximations and enhanced topological skeletons of standard models.

Model	Faces	Feature pts.	Constrict.	Time
Humanoid	1 900	19	9	0.5 s.
Horse 1	20 000	10	11	12 s.
Hand 1	50 000	6	11	75 s.
Hand 2	50 000	6	11	100 s.
Horse 2	40 000	7	19	35 s.

Table 2. Computation times.

8.1. Discussion

Figure 12 presents intermediary results and enhanced topological skeletons of standard models.

Firstly, we can notice that our feature point extraction algorithm achieves correct extractions, even on complex areas, such as the hair of the humanoid model.

Secondly, our constriction approximation algorithm computes nice-looking constrictions (in red in fig. 12) even for coarsely designed objects (figs. 12(f) and 12(g)). It automatically adjusts its detection criterion to the connected component it is processing, enabling the identification of constrictions even on strongly tubular mesh sub-parts (like the legs of the horse models).

Table 1 shows that the number of identified constrictions is quite stable when f_τ varies. The most visually interesting

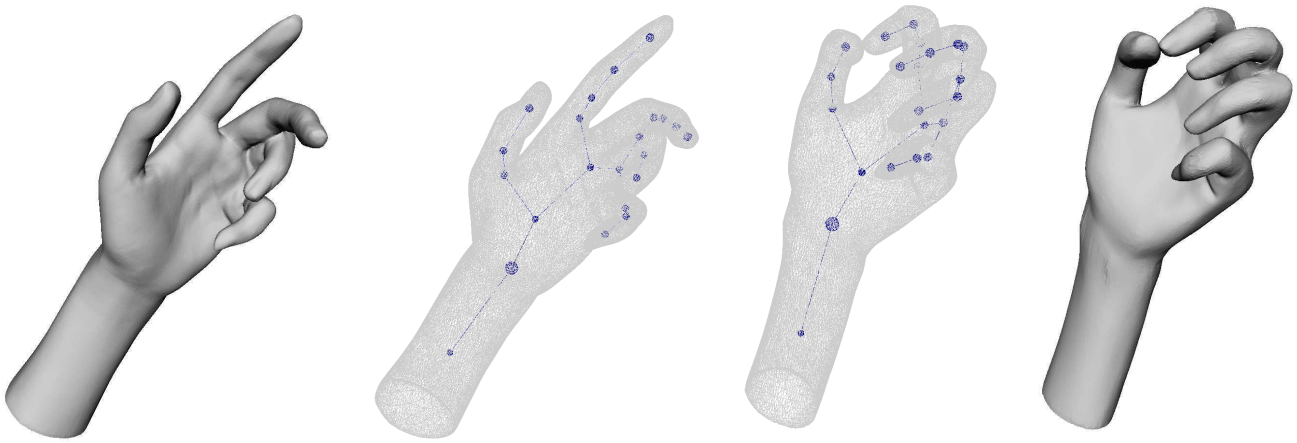

(a) Input mesh. (b) Enhanced topological skeleton. (c) Deformed skeleton. (d) Deformed mesh.

Figure 13. Application to mesh deformation.

results have been obtained setting $f_\tau = 10$. This setting has been chosen for each model in fig. 12.

However, constrictions are approximated assuming they appear along identified discrete contours only. This is a strong hypothesis. As shown in figure 12, thanks to our mapping function definition, this limitation is not detrimental when dealing with natural objects because some contours are actually identified on the articulations of prominent components.

Constriction approximation leads to the subdivision of the branches of the topological skeleton into more visually interesting parts: such as the decomposition of fingers into phalanxes (figs. 12(m) and 12(n)) or the decomposition of legs into thighs, calves and feet (figs. 12(k), 12(l) and 12(o)).

Thanks to f_m invariance properties, those skeletons are invariant to geometrical transformations: translation, rotation and uniform scaling. Furthermore, as shown section 6, thanks to our graph construction strategy, no noisy details are encoded in the skeletons.

8.2. Time complexity

Given an input connected triangulated surface T, let n be the number of vertices in T. Feature point extraction is performed in $O(n \times log(n))$ steps. f_m is computed in $O(|F| \times n \times log(n))$ steps with $|F|$ the number of identified feature points. Notice that f_m has a lower computational cost than the function proposed in [10] ($|F|$ rarely exceeds 20). Each discrete contour computation takes $O(log(n) + n)$. Therefore, as contours are computed for each vertex in T, the overall discrete contour computation takes $O(n^2)$ steps. Topological and geometrical analyses are more straightforward. Topological analysis is performed in $O(n)$ steps. Concavity curves are computed in $O(n)$ steps. Their smoothing is realized in $O(n \times log(n))$, using the Fast Fourier Transform algorithm. Consequently, we can state that the overall complexity of our method is bounded by the discrete contour computation, which takes $O(n^2)$ steps.

Presented algorithms have been implemented in C language under GNU/Linux and experimented on a desktop PC with a 3 GHz P4-CPU and 2 gigabytes of RAM. Table 2 shows the computation times corresponding to the models presented in fig. 12. Notice that our overall method has a significantly lower running time than latest constriction detection [8] or skeleton extraction [24] methods, for equivalently sampled meshes.

8.3. Example of application: mesh deformation

Topological skeletons have shown to benefit various applications in computer graphics [2]. For example, within the framework of shape retrieval, thanks to their invariance properties, enhanced topological skeletons can be used for shape similarity estimation. They are also good supports for shape compression, metamorphosis, texture mapping, etc.

In this paper, to show the usability of our approach, we focus on mesh deformation. Each node of the enhanced topological skeletons references each vertex of the related mesh sub-component. Thus, a novice user can easily apply deformations on selected parts of the object.

Since mesh deformation is not in the scope of this paper, in our experiments, models are deformed by applying simple rotations to components, but more sophisticated strategies can be used [13]. Given an angle and an axis of rotation, a rotation matrix is computed. Then it is applied to each vertex of the selected node, providing nice-looking deformations, as shown in figures 1(f) and 13.

9. Conclusion and future works

In this paper, we presented a fully automatic algorithm for the extraction of affine-invariant enhanced topological skeletons. It first computes a dual Reeb graph. Then it refines it using constrictions as boundaries between mesh subparts. To our knowledge, this is the first approach which unifies Reeb graph and constriction computations.

Our scientific contribution resides in three points. Firstly, we proposed a robust and straightforward feature point extraction algorithm. It enables the computation of an invariant mapping function which reveals well the shape most significant features. Secondly, we presented an algorithm for *discrete contours* computation. We showed that a topological analysis of these *discrete contours* enables a unified Reeb graph construction and simplification process. Resulting graphs do not encode noisy details and they are robust against variations in mesh sampling and invariant to geometrical transformations. Finally, we showed that a geometrical analysis of the *discrete contours* provides nice-looking constriction approximations on prominent components, enabling the refinement of dual Reeb graphs into more visually meaningful skeletons.

Our algorithm computes skeletons with satisfactory execution times, without any input parameter or pre-processing stage. Consequently, it is a good candidate for various applications in computer graphics, like shape deformation (experimented in this paper), retrieval, metamorphosis, compression, texture mapping, etc.

In the future, we would like to experiment more robust geometrical analyses and constriction sliding algorithms, in order to provide more visually interesting skeletons. Moreover, forcing the position of the skeleton inside the object and preserving shape symmetry are enhancements which benefit certain applications and which are currently under investigation.

References

[1] M. Attene, S. Biasotti, and M. Spagnuolo. Shape understanding by contour-driven retiling. *The Visual Computer*, 19:127–138, 2003.

[2] S. Biasotti, S. Marini, M. Mortara, and G. Patanè. An overview on properties and efficacy of topological skeletons in shape modelling. In *Shape Modeling International*, pages 245–254, 2003.

[3] H. Blum and R. N. Nagel. Shape description using weighted symmetric axis features. *Pattern Recognition*, 10:167–180, 1978.

[4] P.-T. Bremer, H. Edelsbrunner, B. Hamann, and V. Pascucci. Topological hierarchy for functions on triangulated surfaces. *IEEE Transactions on Visualization and Computer Graphics*, 10:385–396, 2004.

[5] H. Carr, J. Snoeyink, and M. V. de Panne. Simplifying flexible isosurfaces using local geometric measures. In *IEEE Visualization*, pages 497–504, 2004.

[6] K. Cole-McLaughlin, H. Edelsbrunner, J. Harer, V. Natarajan, and V. Pascucci. Loops in Reeb graphs of 2-manifolds. In *Symposium on Computational Geometry*, pages 344–350, 2003.

[7] H. Edelsbrunner and E. P. Mücke. Simulation of simplicity: a technique to cope with degenerate cases in geometric algorithms. *ACM Transactions on Graphics*, 9:66–104, 1990.

[8] F. Hétroy. Constriction computation using surface curvature. In *Eurographics*, pages 1–4, 2005.

[9] F. Hétroy and D. Attali. From a closed piecewise geodesic to a constriction on a closed triangulated surface. In *Pacific Graphics*, pages 394–398, 2003.

[10] M. Hilaga, Y. Shinagawa, T. Kohmura, and T. Kunii. Topology matching for fully automatic similarity estimation of 3D shapes. In *SIGGRAPH*, pages 203–212, 2001.

[11] S. Katz, G. Leifman, and A. Tal. Mesh segmentation using feature point and core extraction. *The Visual Computer*, 21:865–875, 2005.

[12] F. Lazarus and A. Verroust. Level set diagrams of polyhedral objects. Technical Report 3546, Institut National de Recherche en Informatique et en Automatique (INRIA), 1999.

[13] J. Lewis, M. Cordner, and N. Fond. Pose space deformations: A unified approach to shape. In *SIGGRAPH*, pages 165–172, 2000.

[14] M. Meyer, M. Desbrun, P. Schrder, and A. H. Barr. Discrete differential-geometry operators for triangulated 2-manifolds. In *Visualization and Mathematics*, pages 33–57, 2002.

[15] J. Milnor. *Morse Theory*. Princeton University Press, 1963.

[16] M. Morse. Relations between the critical points of a real function of n independant variables. *Transactions AM. Math. Soc.*, 27:345–396, 1925.

[17] M. Mortara and G. Patanè. Affine-invariant skeleton of 3D shapes. In *Shape Modeling International*, pages 245–252, 2002.

[18] X. Ni, M. Garland, and J. Hart. Fair Morse functions for extracting the topological structure of a surface mesh. *ACM Transactions on Graphics*, 23:613–622, 2004.

[19] G. Reeb. Sur les points singuliers d'une forme de Pfaff complètement intégrable ou d'une fonction numérique. *Comptes-rendus de l'Académie des Sciences*, 222:847–849, 1946.

[20] A. Shamir. A formalization of boundary mesh segmentation. In *IEEE 2nd International Symposium on 3DPVT*, 2004.

[21] P. Shilane, P. Min, M. Kazhdan, and T. Funkhouser. The Princeton shape benchmark. In *Shape Modeling International*, pages 167–178, 2004.

[22] Y. Shinagawa, T. L. Kunii, and Y. L. Kergosien. Surface coding based on morse theory. *IEEE Computer Graphics and Applications*, 11:66–78, 1991.

[23] S. Takahashi, T. Ikeda, Y. Shinagawa, T. L. Kunii, and M. Ueda. Algorithms for extracting correct critical points and constructing topological graphs from discrete geographical elevation data. *Computer Graphics Forum*, 14:181–192, 1995.

[24] F.-C. Wu, W.-C. Ma, R.-H. Liang, B.-Y. Chen, and M. Ouhyoung. Domain connected graph: the skeleton of a closed 3D shape for animation. *The Visual Computer*, 22:117–135, 2006.